J. Fluid Mech. (2026), *vol.* 1033, R2, doi:10.1017/jfm.2026.11439

JFM RAPIDS

Streamwise-localised travelling-wave edge state in square-duct flow

Stanisław Wojciech Gepner[1], **Adrian Wojciech Koźluk**[2], **Shingo Motoki**[2] **and Genta Kawahara**[2]

[1]Warsaw University of Technology, Institute of Aeronautics and Applied Mechanics, Nowowiejska 24, 00-665 Warsaw, Poland

[2]Graduate School of Engineering Science, Osaka University, 1-3 Machikaneyama, Toyonaka, Osaka 560-8531, Japan

Corresponding author: Stanisław Wojciech Gepner, stanislaw.gepner@pw.edu.pl

(Received 6 January 2026; revised 16 February 2026; accepted 11 March 2026)

We report the first streamwise-localised travelling-wave solution in square-duct flow that acts as an edge state in the full phase space, without any imposed spatial symmetries. Performing edge tracking and Newton iteration, we identify a steady travelling wave that possesses a codimension-one stable manifold, which (at least locally) forms the boundary between the basins of laminar and turbulent attractors. Parametric continuation identifies this solution as the lower branch of a saddle-node bifurcation pair. Perturbation analysis places both solutions on the laminar–turbulent boundary and uncovers a heteroclinic connection that links the two branches and is likewise confined to the basin boundary. This symmetry-free, localised edge state expands the catalogue of invariant solutions in wall-bounded shear flows and provides a geometric framework for understanding the transition dynamics in extended systems.

Key words: turbulent transition

1. Introduction

Since Reynolds' 1883 pipe flow experiments (Reynolds 1883), it has been known that flows through circular pipes, narrow rectangular and square ducts can remain laminar well beyond the typical onset of turbulence. These flows exhibit a fundamentally important phenomenon known as subcritical transition: the laminar state is linearly stable, and turbulence arises only through finite-amplitude perturbations. As a result, laminar and turbulent states coexist in the phase space, separated by the attraction basin boundary known as the edge. From a dynamical systems perspective, departures from the laminar solution – including turbulence – correspond to trajectories in a high-dimensional phase space structured by unstable invariant solutions – such as travelling waves (relative equilibria), periodic orbits, relative periodic orbits (RPOs) or more complex chaotic invariant sets, including chaotic edge dynamics (Duguet, Willis & Kerswell 2008; Brynjell-Rahkola, Duguet & Boeck 2025; Weyrauch, Uhlmann & Kawahara 2025) – that emerge via saddle-node bifurcations (Waleffe 1998; Kawahara, Uhlmann & van Veen 2012). Among these, edge states – solutions with codimension-one stable manifolds – play a central role in the transition dynamics by separating initial conditions that decay to laminar flow from those that evolve into turbulence. In this work, we look for solutions that are simple relative equilibria, located on the edge, since such solutions, in contrast to the more complex (chaotic) counterparts (Weyrauch *et al.* 2025), allow for characterisation of their dynamics, continuation and stability evaluation.

The significance of edge states in organising the transitional dynamics extends to a broad class of nonlinear, dissipative systems with multiple coexisting attractors, from fluid dynamics, climate and ecological models to magnetohydrodynamic shear flows subject to strong magnetic damping (Kawahara *et al.* 2012; Lucarini & Bódai 2019; Wieczorek, Xie & Ashwin 2023; Brynjell-Rahkola *et al.* 2025). In such cases, edge states define the system's basin boundaries through their stable, codimension-one manifolds, on which they act as relative attractors, separating initial conditions that lead to distinct long-term outcomes. Identifying edge states enables precise determination of the disturbance shape and amplitude required to trigger transitions (Kawahara 2005), offering potential strategies for sustaining desirable states or avoiding undesired ones. Moreover, edge states provide a framework for anticipating tipping points, as trajectories influenced by fluctuations tend to approach the edge manifold before shifting to a new attractor (Wieczorek *et al.* 2023; Brynjell-Rahkola, Duguet & Boeck 2024). The discovery of edge states is therefore essential for understanding the transition dynamics in high-dimensional, nonlinear systems not restricted to fluid mechanics.

In transitional shear flows, turbulence often appears as spatially localised spots (planar flows) or puffs (pipe and duct flows) embedded in a laminar background, so spatially localised edge states are of particular interest (Graham & Floryan 2021). For pipe and square-duct flows, the emergence and dynamics of puffs have been analysed in detail (Barkley *et al.* 2015; Graham 2015; Barkley 2016) with numerical results connecting puff formation to the dynamics of the spatially localised solution pair (Budanur & Hof 2017), and in planar flows, spot nucleation was connected to localised edge states (Schneider, Marinc & Eckhardt 2010; Graham & Floryan 2021). Still, identified localised solutions remain rare. In pipe flow, streamwise-localised, RPO solutions have been found, but their lower branches (LBs) do not act as edge states without symmetry constraints (Avila *et al.* 2013; Chantry, Willis & Kerswell 2014). In square-duct flow, localised solutions are even scarcer. Several domain-filling solutions have been linked to square-duct turbulence statistics (Wedin, Bottaro & Nagata 2009; Okino *et al.* 2010; Weyrauch *et al.* 2025) and the first edge-tracking study in this geometry was carried out by Biau & Bottaro (2009), but only one streamwise-localised solution pair has been reported so far (Gepner, Okino & Kawahara 2025). This pair has a form of four vortices placed in pairs at opposite walls, and its LB acts as an edge state only within a π-rotational symmetric subspace. Without symmetry constraints, this LB appears embedded in the turbulent attractor and experiences occasional approaches by the turbulent flow state (Gepner *et al.* 2025) during intermittent quiescent episodes accompanied by structure localisation. To the best of the authors' knowledge, no localised simple edge state has yet been discovered in the full phase space of the circular pipe or square-duct flow without any spatial symmetries.

The early square-duct edge-tracking computations, performed in a short, streamwise periodic domain (Biau, Soueid & Bottaro 2008; Biau & Bottaro 2009) already suggested that in a short duct the laminar–turbulent boundary is organised by a domain-filling, wall-attached streak-vortex structures. In particular, Biau & Bottaro (2009) reported a chaotic edge, whose cross-sectional organisation is represented by a two-vortex state, i.e. a pair of counter-rotating streamwise vortices associated with a low-velocity streak over one of the four walls, with the active wall alternating in time. More recently, Weyrauch *et al.* (2025) showed that, in the full (unconstrained) phase space, the edge dynamics can take the form of a chaotic attractor, typically featuring long quiescent phases dominated by a single low-speed streak with flanking vortices attached to one wall, accompanied by bursting events that trigger a switch of activity to a neighbouring wall. They further argue that analogous two-vortex (single-wall) episodes observed in marginally turbulent duct flow can be interpreted as transient visits to such edge states. The travelling wave reported here can be viewed as a streamwise-localised invariant realisation of this single-wall streak-vortex dynamics.

In this work, we report the first streamwise-localised simple travelling-wave solution in square-duct flow, which acts as an edge state in the full phase space and is free of symmetry restrictions. Contrary to the sub-space, four-vortex edge state reported in Gepner *et al.* (2025), this new solution has the form of a single vortex pair localised near only one of the duct walls, meaning it is more confined in the cross-axial direction and, at sufficiently high Reynolds number, further apart from the turbulent saddle. To obtain this solution, we combine edge tracking via bisection (Itano & Toh 2001; Skufca, Yorke & Eckhardt 2006) with a Newton–Krylov solver (Viswanath 2007, 2009) and Arnoldi-based linear stability analysis in a spectral element method (SEM) framework, and identify a travelling-wave solution whose LB possesses a codimension-one stable manifold, confirming its role as an edge state in the full phase space. We then characterise this solution by continuation and linear stability analysis, and test the unstable directions to establish its role on the laminar–turbulent boundary.

2. Problem statement

We consider an incompressible Newtonian fluid flow through a square duct with walls located at cross-axial positions $x = \pm h$ and $y = \pm h$, and periodic in the axial z-direction with period L_z. Unless stated otherwise, $L_z = 8\pi h$, which is close to the minimal streamwise length suitable for supporting the previously reported localised solution (Okino 2014; Gepner *et al.* 2025). The flow, represented by the velocity vector $\boldsymbol{u} = [u, v, w]$, is driven by a constant-in-time pressure gradient producing a laminar flow $\boldsymbol{u}_l$ with a steady, quasi-parabolic velocity profile. We use the half-width h of the duct as the characteristic length scale, and the laminar centreline velocity W for the given constant-in-time streamwise pressure gradient as the characteristic velocity scale to non-dimensionalise physical quantities. Taking density ρ as unity and kinematic viscosity ν, the Reynolds number is defined as $Re = Wh/\nu$ and the bulk Reynolds number is $Re_b(t) = w_b(t)h/\nu$, with $w_b(t) = (1/V)\iiint_V w(t)\,\mathrm{d}V$ where V is the domain volume. Due to the applied pressure gradient constraint, Re_b is not a fixed quantity – see table 1.

The system is studied via the SEM implemented in Nektar++ (Cantwell *et al.* 2015; Moxey *et al.* 2020). The numerical resolution matches that used by Gepner *et al.* (2025), comprising four quadrilateral elements in the (x, y)-plane, each with polynomial order $p = 24$ and $q = 36$ Gauss–Lobatto–Legendre quadrature points per direction, satisfying

	Turbulent	Laminar	LB ($L_z = 8\pi$)	LB ($L_z = 32\pi$)	UB ($L_z = 8\pi$)
$\langle Re_b \rangle$	1136	1908	1901	1907	1780
$\langle w_b \rangle$	0.2839	0.4770	0.4752	0.4768	0.4495
$\langle f \rangle$	0.0424	0.0149	0.0151	0.0150	0.0168
σ	—	—	0.0372	0.0371	Multiple

Table 1. Time-averaged flow quantities and growth rate σ of the leading eigenmode (if applicable) for different types of solutions at $Re = 4000$. Here, $\langle \cdot \rangle$ indicates a time-averaged value.

the $q = 3/2p$ integration rule for exact nonlinear term quadrature (Karniadakis *et al.* 2005). In the streamwise z-direction, a Fourier discretisation is employed, truncated to $M = \pm 128$ modes prior to applying the 2/3 dealiasing rule (Patterson Jr & Orszag 1971). The resulting spatial resolution corresponds to approximately 1.8×10^6 degrees of freedom (DoF) for velocity components. Robustness is confirmed by increasing the resolution to $p = 30$, $q = 45$ and $M = \pm 144$ ($\sim 3.1 \times 10^6$ DoF), which yields consistent invariant solution characteristics and stability properties.

3. Edge tracking

Perturbing the laminar flow with a short (approximately 2 time units) low-intensity white-noise body force (volume forcing) applied to the momentum equations induces a non-laminar dynamics. Depending on the Reynolds number and the disturbance amplitude, this non-laminar response manifests itself either as a chaotic transient, eventually relaminarising, or as sustained turbulence. At $Re = 4000$, we observe a persistent non-laminar state; throughout long-time simulations exceeding 10^5 time units, no return to laminar flow is detected. Conversely, below approximately $Re = 3600$, only transient non-laminar states arise, with relaminarisation typically occurring within 10^4 time units. This suggests the presence of a critical Reynolds number for sustained turbulence in the square duct, akin to previous observations in pipe flow (Avila *et al.* 2011). Below this threshold, turbulence is transient (a chaotic saddle dynamics), and the notion of the edge should be understood as the codimension-one boundary separating initial conditions that relaminarise directly from those that first undergo chaotic transients (Chantry *et al.* 2014). For subsequent edge-tracking analysis, we fix the Reynolds number at $Re = 4000$, corresponding to a friction Reynolds number $Re_\tau \approx 82$, and the laminar and time-averaged turbulent bulk Reynolds numbers are equal to $Re_b = 1908$ and $\langle Re_b \rangle = 1136$, respectively, with $\langle \cdot \rangle$ indicating a time-averaged value (see table 1).

We initiate edge tracking with a snapshot $\boldsymbol{u}_s$ drawn from fully developed turbulent flow. This snapshot is taken sufficiently far from the initial perturbation (2000 time units later or even longer) to ensure it originates from the turbulent attractor rather than the transient phase. No additional criteria are imposed in selecting the initial condition for edge tracking. We then apply the classical bisection algorithm (Itano & Toh 2001; Skufca *et al.* 2006) to find initial states $\boldsymbol{u}_i = \boldsymbol{u}_l + \alpha(\boldsymbol{u}_s - \boldsymbol{u}_l)$, varying $\alpha \in (0, 1)$ at time $t = 0$ such that the flow neither relaminarises nor transitions fully to turbulence but remains on the laminar–turbulent boundary, the edge, separating the two attraction basins. During the bisection process, both the perturbation energy $E_{3D} = (1/2V) \sum_{k=1}^{M} \iiint_V \boldsymbol{u}_{-k} \cdot \boldsymbol{u}_k \, \mathrm{d}V$ and the friction factor $f = 8(Re_\tau / Re_b)^2$ are monitored and gradually decrease from their turbulent values, while exhibiting recurrent fluctuations.

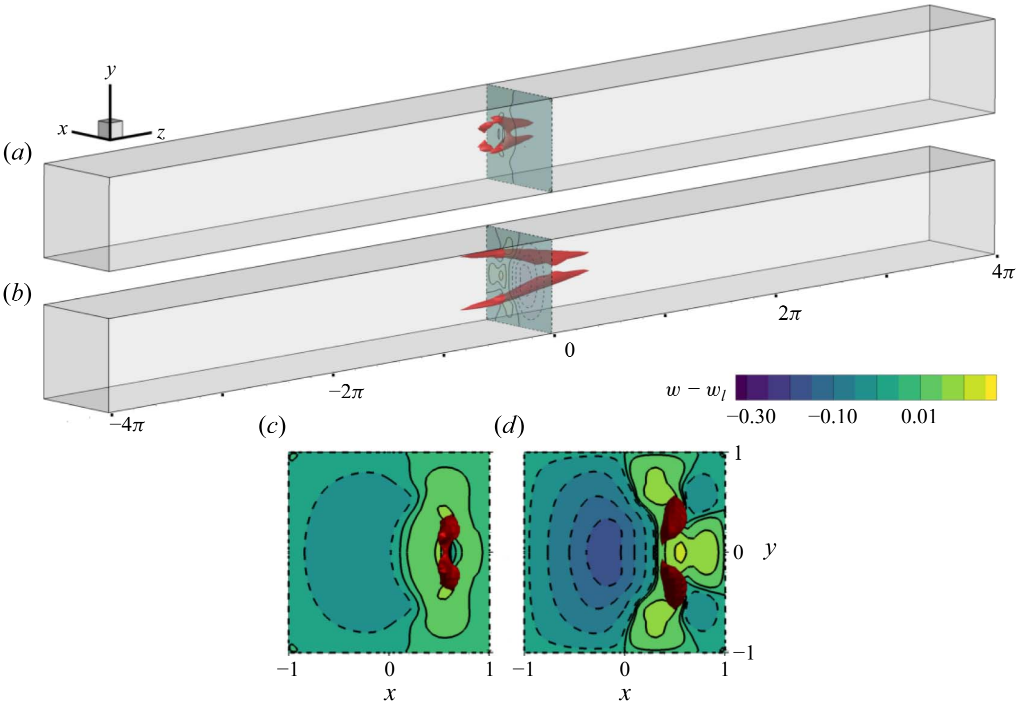

Figure 1. Snapshots of the velocity field depicting (a,c) the identified edge state – LB solution – and (b,d) the upper branch (UB) solution at $Re = 4000$. Panels (a,b) show isosurfaces of the second invariant of the velocity gradient tensor Q at 0.01, and panels (c,d) display contours of the difference in the streamwise-velocity component w relative to the laminar solution w_l, with negative values indicated by dashed lines; all slices are taken at $z = 0$. Velocity fields are adjusted such that the maximum velocity perturbation aligns with $z = 0$.

This bisection process has been implemented starting from various initial snapshots, with some leading the procedure to converge, after an initial transient, to a regular state with a non-zero asymptote of perturbation energy. The velocity field obtained via bisection was then used as an initial guess for a custom implementation of the Newton–Krylov solver (Viswanath 2007, 2009) built around the Nektar++ framework. The solver converged to a simple travelling-wave solution. During independent bisections, we observe convergence to the same regular travelling-wave solution, up to a rotation by $\pi/2$ about the duct axis. This is consistent with the $\pi/2$-rotational equivariance of the square-duct geometry, implying that symmetry-related copies can be located at any wall.

This solution features a streamwise-localised vortex pair situated next to one wall of the duct (here shown at $x = 1$) that travels downstream at a constant phase speed $w_p = 0.695$. Figure 1(a,c) illustrates the invariant solutions via $Q = (1/2)(\|\varOmega\|^2 - \|S\|^2)$ contours (Hunt, Wray & Moin 1988), with S and $\varOmega$ the symmetric and antisymmetric parts of the velocity gradient tensor, respectively, plotted at $Q = 1.0 \times 10^{-2}$, and streamwise-velocity perturbations relative to the laminar quasi-parabolic profile on the $z = 0$ plane. While the computations are performed in the full phase space without imposing any symmetry constraints, the converged travelling wave exhibits an autonomous reflection symmetry with respect to one of the wall bisectors – here $y = 0$ (see figure 1), illustrating that symmetries arise autonomously even in the full, unconstrained phase space.

To investigate streamwise localisation, we continued the solution by increasing the domain length L_z, maintaining $Re = 4000$ and adjusting the streamwise resolution to

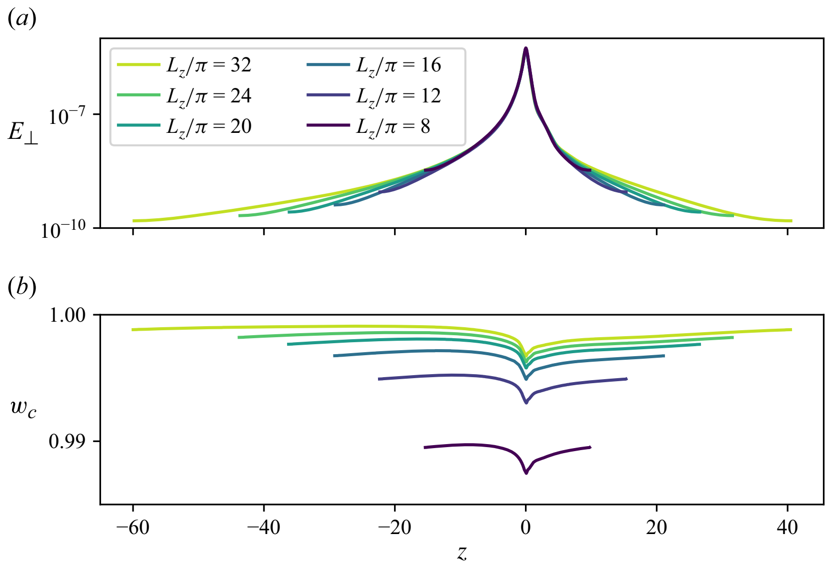

Figure 2. Variations of (*a*) the cross-flow energy $E_\perp$ and (*b*) streamwise velocity at the duct centre w_c of the LB solution at $Re = 4000$ with streamwise coordinate z. Velocity fields are shifted in the periodic z-direction such that the maximum cross-flow energy is located at $z = 0$.

preserve approximately 10 Fourier modes per unit length. Figure 2(*a*) shows the streamwise variation of the cross-flow energy $E_\perp(z) = (1/4)\int_{-1}^{1}\int_{-1}^{1}(1/2)(u^2 + v^2)\,\mathrm{d}x\,\mathrm{d}y$, and figure 2(*b*) the centreline streamwise-velocity w_c, for increasing periodic length L_z, illustrating that the cross-flow energy remains confined around a compact core as L_z is increased, whereas the streamwise-velocity perturbation exhibits weaker, non-exponential decay. In this sense, streamwise localisation refers to the energy core (based on $E_\perp(z)$) rather than implying strict exponential localisation in all velocity components. This trend suggests that, with further increase of the domain length, the solution should persist and remain available for the case of a fully extended system, making it meaningful for experimental investigation (De Lozar *et al.* 2012).

Using the arc-length continuation method (Keller 1977; Dijkstra *et al.* 2014), we continued the solution in Reynolds number while keeping the domain length fixed at $L_z = 8\pi$. This continuation revealed that the identified edge state corresponds to the LB of a saddle-node bifurcation occurring near $Re = 2794.5$. We further identified the corresponding UB solution of this pair and continued it with increasing Reynolds number. Figure 1(*b*,*d*) illustrates the UB topology at $Re = 4000$. Similarly, by fixing $Re = 4000$ and varying the duct length L_z, we observed an analogous saddle-node bifurcation near $L_z \approx 4.64\pi$, with an associated UB solution. At $L_z = 8\pi$, the UB solution matches that shown in figure 1(*b*,*d*). These results confirm that the identified solution belongs to a continuous solution branch parametrised by both Reynolds number and domain length.

Stability analysis of the identified solution pair was conducted using Arnoldi iterations (Viswanath 2009). At $Re = 4000$ and $L_z = 8\pi$, the LB solution possesses a single purely real unstable eigenvalue (see table 1) in the full phase space, confirming its status as an edge state. Accordingly, this travelling wave represents a full-phase-space edge state whose codimension-one stable manifold locally partitions the phase space into two distinct basins (Duguet *et al.* 2008; Gepner *et al.* 2025), thus forming the laminar–turbulent edge. Unlike the previously reported symmetric-subspace edge states in square-duct flow (Okino 2014;

Gepner *et al.* 2025) and pipe flow (Avila *et al.* 2013) – both appearing embedded within the turbulent attractor (Avila *et al.* 2013; Gepner *et al.* 2025) – the present solution is necessarily separated from the turbulent trajectory, a prerequisite for persistent turbulence (Lustro *et al.* 2019). Extending the stability analysis to longer domains reveals that the identified travelling wave remains an edge state for streamwise lengths of at least $L_z = 32\pi$ (>100), the longest domain length considered here, with only small variation in the growth rate of the single unstable eigenvalue, suggesting that it should be an edge state in a fully extended system.

4. Edge-state continuation and heteroclinic connection

The performed stability analysis shows that the LB solution remains an edge state, possessing a single unstable eigenvalue across all tested Reynolds numbers up to the bifurcation point at $Re = 2794.5$. The coexisting UB solution has multiple unstable directions. Past the bifurcation point, for Reynolds numbers in the range $Re \in (2794.5, 2800)$, the UB solutions feature precisely two real unstable eigenvalues. Beyond $Re = 2800$, up to at least $Re = 2823$, the number of real unstable eigenvalues increases to three. Prior to $Re = 2847$, two of these real unstable eigenvalues transition into a pair of complex conjugate unstable eigenvalues. Additional unstable eigenvalues continue to appear on the UB as the Reynolds number is further increased.

The single purely real unstable eigenvalue of the LB solution defines a direction necessarily transverse to the edge manifold (Duguet *et al.* 2008) at the LB. In contrast, for Reynolds numbers below approximately 2800, the UB solution possesses two purely real unstable eigenvalues, which locally define a two-dimensional unstable manifold. We investigate unstable directions of both branches by perturbing the LB solution along its single unstable eigenvector and the UB solutions in a direction that is a combination of its two unstable eigenvectors at $Re = 2796$ and $L_z = 8\pi$. The resulting trajectories are shown in figure 3 in the (E_{3D}, f)-plane. In each case, the separation of initial conditions is clear between those that relaminarise and those that transition to turbulence. By performing bisection along unstable directions, we track edge trajectories that start near these solutions. For the LB, initial conditions lie increasingly longer near the solution before departing toward either laminar or turbulent states, confirming its role as an edge state. A similar pattern occurs for the UB when perturbed along its leading unstable direction, suggesting this direction remains closely transverse to the edge. At the same time, perturbations that are closely aligned with the secondary unstable eigenvector of the UB, with only a small component along the leading unstable eigenvector (see the inset in figure 3) initially depart but remain confined to the edge. As bisection progresses, trajectories starting at UB steadily approach the LB, as depicted by the a thick arrow in the inset in figure 3. This bisection exhibits recurrent escapes to laminar or turbulent states, consistent with trajectories embedded within the edge manifold. Ultimately, the bisection converges to the LB solution, exhibiting monotonic decay in perturbation energy and friction factor. A final Newton iteration confirms that the approached state is the LB solution and providing sound evidence for a heteroclinic connection embedded in the edge, which links the UB and LB solutions. Consequently, the UB solution must also reside within this edge (but is not an edge state itself).

5. Conclusions

We have identified a fully localised travelling-wave edge state in the full (symmetry-unconstrained) phase space. Its codimension-one stable manifold forms, at least locally,

https://doi.org/10.1017/jfm.2026.11439 Published online by Cambridge University Press

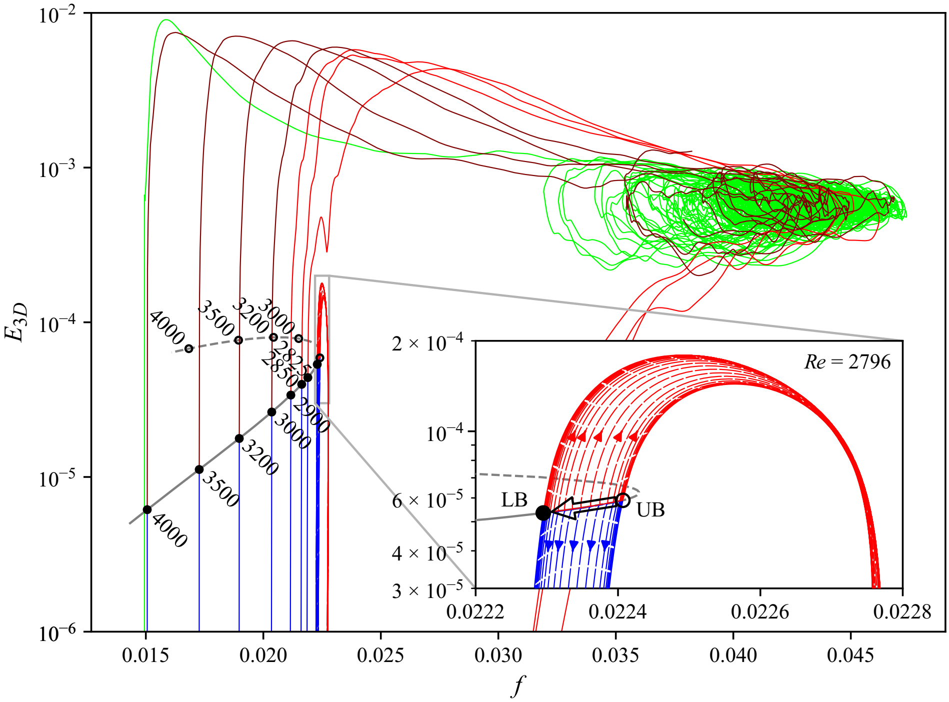

Figure 3. State portrait of the dynamics represented on the $(E_{3D},\ f)$-plane. The green solid curve corresponds to a persistent turbulent trajectory at $Re = 4000$, observed over 10^5 time units. The grey solid (dashed) line represents the LB (UB) solutions with varying Reynolds number. Solid red (blue) curves start from edge states at different Re and depict excursions toward the turbulent attractor (if one exists) – solid dark red – or the turbulent transient – solid red – (laminarisation) generated from initial conditions formed by perturbing the LB and UB within their respective unstable manifolds. Red and blue curves shown in the inset depict the bisection process started from the UB solution, following the heteroclinic orbit (marked with a thick arrow) connecting the UB to the LB solution at $Re = 2796$.

a subset of the laminar–turbulent boundary, which may consist of multiple (possibly disconnected) components and host multiple edge states. This newly discovered solution consists of a single streamwise vortex pair localised near only one duct wall, i.e. it is more confined in the cross-axial direction than the four-vortex solution reported earlier in Gepner *et al.* (2025) and consequently, in the phase space, it lies further from the turbulent attractor.

The appearance of such a two-vortex organisation is consistent with earlier observations of the transitional square-duct flow in the short streamwise periodic domain by Biau *et al.* (2008), who reported that trajectories near the threshold can visit states with only two large-scale vortex pairs near opposing walls and may approach even simpler vortex configurations, like the two-vortex state, just prior to relaminarisation. Likewise, the edge-tracking study of Biau & Bottaro (2009) found an edge trajectory organised around the two-vortex state exhibiting intermittent wall switching, suggesting that low-dimensional wall-attached vortex pairs may serve as building blocks for a more complex edge dynamics.

Our localised, simple travelling-wave edge state provides a geometric characterisation of the basin boundary, which is crucial for quantifying the disturbance amplitude and shape required for effective transition control. The streamwise localisation of the identified edge state ensures its relevance to fully extended flow domains or experimental verification.

Via continuation and stability analysis, we have shown that this solution forms the LB of a saddle-node pair, with the UB exhibiting a two-dimensional unstable manifold, for a range of Reynolds numbers. Our perturbation analysis reveals a heteroclinic connection embedded within the edge manifold and linking the UB to the LB solutions. This fact underlines that both solution branches remain on the edge, at least close to the bifurcation point. The identified connection provides insight into the geometry of a portion of the laminar–turbulent boundary in the system, where no symmetry restrictions are applied The persistence of the LB as an edge state across a range of Reynolds numbers and domain lengths supports its importance in organising the transition dynamics in square-duct flow.

Finally, the present results can be viewed as complementary to recent long-time studies of the edge dynamics. In particular, Weyrauch *et al.* (2025) showed that, in the full (non-symmetric) phase space, edge trajectories can display a chaotic dynamics with alternating quiescent intervals and bursting episodes, typically localised to one wall and accompanied by wall switching, while symmetry restrictions can yield travelling-wave edge states. Within this picture, the fully localised LB travelling wave reported here provides a minimal invariant state that is possibly linked to the quiescent phases, constituting a natural base point for computations of connections between steady travelling waves, RPOs and chaotic invariant sets embedded in the edge manifold. Establishing whether (and how) chaotic wall-switching edge trajectories organise around repeated approaches to this LB state, and how the identified heteroclinic connection interacts with the bursting dynamics, are promising directions for further work.

Acknowledgements. The authors acknowledge the support of the Interdisciplinary Centre for Mathematical and Computational Modelling at the University of Warsaw (ICM UW) for providing computational resources and infrastructure.

Funding. This work was supported by the Japan Society for the Promotion of Science (JSPS) through the FY2020 JSPS Postdoctoral Fellowship for Research in Japan (Short-term), Grant No. PE20715, and by the National Science Centre, Poland, under the Sonata-15 program (Grant No. 2019/35/D/ST8/00090).

Declaration of interests. The authors report no conflicts of interest.

Data availability statement. The data supporting this study's findings are available from the corresponding author upon reasonable request.

References

AVILA, K., MOXEY, D., DE LOZAR, A., AVILA, M., BARKLEY, D. & HOF, B. 2011 The onset of turbulence in pipe flow. *Science* **333** (6039), 192–196.

AVILA, M., MELLIBOVSKY, F., ROLAND, N. & HOF, B. 2013 Streamwise-localized solutions at the onset of turbulence in pipe flow. *Phys. Rev. Lett.* **110** (22), 224502.

BARKLEY, D. 2016 Theoretical perspective on the route to turbulence in a pipe. *J. Fluid Mech.* **803**, P1.

BARKLEY, D., SONG, B., MUKUND, V., LEMOULT, G., AVILA, M. & HOF, B. 2015 The rise of fully turbulent flow. *Nature* **526** (7574), 550–553.

BIAU, D. & BOTTARO, A. 2009 An optimal path to transition in a duct. *Phil. Trans. R. Soc. A: Math. Phys. Engng Sci.* **367** (1888), 529–544.

BIAU, D., SOUEID, H. & BOTTARO, A. 2008 Transition to turbulence in duct flow. *J. Fluid Mech.* **596**, 133–142.

BRYNJELL-RAHKOLA, M., DUGUET, Y. & BOECK, T. 2024 Chaotic edge regimes in magnetohydrodynamic channel flow: an alternative path towards the tipping point. *Phys. Rev. Res.* **6** (3), 033066.

BRYNJELL-RAHKOLA, M., DUGUET, Y. & BOECK, T. 2025 Route to turbulence in magnetohydrodynamic square duct flow. *Phys. Rev. Fluids* **10** (2), 023903.

BUDANUR, N.B. & HOF, B. 2017 Heteroclinic path to spatially localized chaos in pipe flow. *J. Fluid Mech.* **827**, R1.

CANTWELL, C.D., *et al.* 2015 Nektar++: an open-source spectral/ element framework. *Comput. Phys. Commun.* **192**, 205–219.

Chantry, M., Willis, A.P. & Kerswell, R.R. 2014 Genesis of streamwise-localized solutions from globally periodic traveling waves in pipe flow. *Phys. Rev. Lett.* **112** (16), 164501.

De Lozar, A., Mellibovsky, F., Avila, M. & Hof, B. 2012 Edge state in pipe flow experiments. *Phys. Rev. Lett.* **108** (21), 214502.

Dijkstra, H.A., *et al.* 2014 Numerical bifurcation methods and their application to fluid dynamics: analysis beyond simulation. *Commun. Comput. Phys.* **15** (1), 1–45.

Duguet, Y., Willis, A.P. & Kerswell, R.R. 2008 Transition in pipe flow: the saddle structure on the boundary of turbulence. *J. Fluid Mech.* **613**, 255–274.

Gepner, S.W., Okino, S. & Kawahara, G. 2025 Streamwise-localised, symmetric invariant solutions in square-duct flow. *J. Fluid Mech.* **1016**, A54.

Graham, M.D. 2015 Turbulence spreads like wildfire. *Nature* **526** (7574), 508–509.

Graham, M.D. & Floryan, D. 2021 Exact coherent states and the nonlinear dynamics of wall-bounded turbulent flows. *Annu. Rev. Fluid Mech.* **53**, 227–253.

Hunt, J.C.R., Wray, A.A. & Moin, P. 1988 Eddies, streams, and convergence zones in turbulent flows. In *Proceedings of the 1988 Summer Program, Center for Turbulence Research*, pp. 193–208. NASA Ames/Stanford University.

Itano, T. & Toh, S. 2001 The dynamics of bursting process in wall turbulence. *J. Phys. Soc. Japan* **70** (3), 703–716.

Karniadakis, G.E. & Sherwin, S.J. 2005 *Spectral/Hp Element Methods for Computational Fluid Dynamics*. Oxford University Press.

Kawahara, G. 2005 Laminarization of minimal plane Couette flow: going beyond the basin of attraction of turbulence. *Phys. Fluids* **17** (4), 041702.

Kawahara, G., Uhlmann, M. & van Veen, L. 2012 The significance of simple invariant solutions in turbulent flows. *Annu. Rev. Fluid Mech.* **44**, 203–225.

Keller, H.B. 1977 Numerical solution of bifurcation and nonlinear eigenvalue problem. In *Application of Bifurcation Theory* (ed. P. Rabinowitz), pp. 359–384. Academic Press.

Lucarini, V. & Bódai, T. 2019 Transitions across melancholia states in a climate model: reconciling the deterministic and stochastic points of view. *Phys. Rev. Lett.* **122** (15), 158701.

Lustro, J.R.T., Kawahara, G., van Veen, L., Shimizu, M. & Kokubu, H. 2019 The onset of transient turbulence in minimal plane Couette flow. *J. Fluid Mech.* **862**, R2.

Moxey, D., *et al.* 2020 Nektar++: enhancing the capability and application of high-fidelity spectral/hp element methods. *Comput. Phys. Commun.* **249**, 107110.

Okino, S. 2014 Spatially localized solutions in rectangular duct flow. In *Prodeedings of JSME FED Meeting 2014*, pp. 0802. JSME.

Okino, S., Nagata, M., Wedin, H. & Bottaro, A. 2010 A new nonlinear vortex state in square-duct flow. *J. Fluid Mech.* **657**, 413.

Patterson Jr, G.S. & Orszag, S.A. 1971 Spectral calculations of isotropic turbulence: efficient removal of aliasing interactions. *Phys. Fluids* **14** (11), 2538–2541.

Reynolds, O. 1883 III. An experimental investigation of the circumstances which determine whether the motion of water shall be direct or sinuous, and of the law of resistance in parallel channels. *Proc. R. Soc. Lond.* **35** (224–226), 84–99.

Schneider, T.M., Marinc, D. & Eckhardt, B. 2010 Localized edge states nucleate turbulence in extended plane Couette cells. *J. Fluid Mech.* **646**, 441–451.

Skufca, J.D., Yorke, J.A. & Eckhardt, B. 2006 Edge of chaos in a parallel shear flow. *Phys. Rev. Lett.* **96** (17), 174101.

Viswanath, D. 2007 Recurrent motions within plane Couette turbulence. *J. Fluid Mech.* **580**, 339–358.

Viswanath, D. 2009 The critical layer in pipe flow at high Reynolds number. *Phil. Trans. R. Soc. A: Math. Phys. Engng Sci.* **367** (1888), 561–576.

Waleffe, F. 1998 Three-dimensional coherent states in plane shear flows. *Phys. Rev. Lett.* **81** (19), 4140.

Wedin, H., Bottaro, A. & Nagata, M. 2009 Three-dimensional traveling waves in a square duct. *Phys. Rev. E* **79** (6), 065305.

Weyrauch, M., Uhlmann, M. & Kawahara, G. 2025 Chaotic and time-periodic edge states in square duct flow. *J. Fluid Mech.* **1021**, A40.

Wieczorek, S., Xie, C. & Ashwin, P. 2023 Rate-induced tipping: thresholds, edge states and connecting orbits. *Nonlinearity* **36** (6), 3238.